Hindawi
Shock and Vibration
Volume 2019, Article ID 6052745, 13 pages
https://doi.org/10.1155/2019/6052745

Research Article

Comparative Study on Dynamic Response of Deck Pavement of Two Kinds of Box Girder Bridges under Moving Loads

Chundi Si,[1,2] Xin Su,[1,3] Enli Chen,[1,2] and Zhanyou Yan[1,3]

[1]*State Key Laboratory of Mechanical Behavior in Traffic Engineering Structure and System Safety, Shijiazhuang Tiedao University, Shijiazhuang 050043, Hebei, China*
[2]*Key Laboratory of Traffic Safety and Control of Hebei Province, Shijiazhuang Tiedao University, Shijiazhuang 050043, Hebei, China*
[3]*School of Civil Engineering, Shijiazhuang Tiedao University, Shijiazhuang 050043, Hebei, China*

Correspondence should be addressed to Xin Su; 18333198309@163.com

Received 18 March 2019; Accepted 24 July 2019; Published 2 September 2019

Academic Editor: Francesco Franco

The objective of this study is to analyse the difference of dynamic response of the deck pavement between a box girder bridge with corrugated steel webs and a concrete web box girder bridge. In this study, a simply supported beam with a span of 34 m is taken as the research object. According to the principle of equal shear stress of the box girder section, the three-dimensional finite element model of the superstructure of two kinds of box girder bridges is established by the finite element software ABAQUS. The DLOAD and UTRACLOAD subroutines are called to impose a movement load on the bridge deck. The dynamic response of the bridge deck pavement under different vehicle speeds (36 km/h, 72 km/h, and 108 km/h) and different load types (single wheel rectangular uniform load and double wheel rectangular uniform load) is calculated. The variation trends of vertical displacement, longitudinal shear stress, and transverse stress of two bridges are compared. The results show that, under the same conditions, the dynamic response of the box girder bridge with corrugated steel webs is greater than that of the equivalent concrete web box girder bridge. The box girder bridge with corrugated steel webs has lightweight, good seismic performance and bending resistance, and more obvious advantages in deflection control. The equivalent concrete web box girder bridge has good shear and torsional properties. The response of two kinds of deck pavement systems of the box girder bridge under dynamic loads is more obvious than that under static loads. This study would provide some theoretical reference for the dynamic response of the deck paving system of box girder bridges.

1. Introduction

Along with the rapid development of science, technology, and national economy, there are more and more types of bridges, the speed of vehicles has been greatly improved, and the number of multiaxle and heavy-haul vehicles has significantly increased. Thus, the damage of the bridge structure pavement system became increasingly complex and prominent. At present, many scholars in China and other countries around the world have studied static and dynamic characteristics of different types of bridges and have obtained a lot of research results.

Based on the theory of the elastic layered systems, Castro [1] studied and analysed two hypotheses of complete bond and complete slip between the pavement and concrete bridge decks by using a circular vertical load. The T-girder, box girder, and full-thickness slab beam were calculated, the maximum stress and strain at the bottom of the asphalt pavement were analysed, and the fatigue calculation formula of the pavement was given. Fiore and Marano [2] conducted full-scale ambient vibration tests involving a 380 m concrete box girder bridge and compared the measured results of environmental vibration with the modal frequencies calculated by a detailed three-dimensional finite element model

of the bridge. The results show that the linear finite element model can accurately reflect the dynamic characteristics of the concrete box girder bridge. Choi et al. [3] conducted an extensive parametric study to determine the maximum stress, deflection, and moment distribution factors for two span multicell box girder bridges based on a finite element analysis of 120 representative numerical model bridges. A set of equations proposed to describe the properties of such bridges under AASHTO LRFD live loads yielded results that agreed closely with the numerically derived results for the stress and deflection distribution factors. Sang-Youl and Sung-Soon [4] conducted a three-dimensional dynamic analysis of the simply supported box beam subjected to moving loads, using four-node Lagrangian and Hermite finite elements. A good agreement was obtained between the numerical solution and the experimental data. Du [5, 6] analysed the stress response of the concrete box girder bridge deck pavement under moving loads, studied the influence of different speeds and overload levels on the mechanical indexes of the flexible bridge deck pavement layer, and proposed that the surface of the bridge deck pavement layer was affected. Mohseni et al. [7] studied the dynamic characteristics of multicell box girder bridges under moving loads. Dynamic impact factor expressions for skew bridges were deduced based on upper-bound values of obtained results. The comparisons indicated that the current bridge codes are unable to estimate accurate values for dynamic responses of skew bridges. In order to fully understand the properties of steel web girders and the effects of steel web connection joints, Jung et al. [8] conducted a static loading test on five prestressed concrete hybrid girders with steel web members and compared the structural safety and service performance. Considering the tensile characteristics of concrete, Ko et al. [9] established an improved analytical model for torsion of the composite box girder with corrugated steel webs and compiled a nonlinear torsional analysis program for torsion of the composite box girder with corrugated steel webs. The program results were compared with the experimental results, and the correctness of the program was verified. Based on the asphalt pavement structure of the box girder bridge with corrugated steel webs, Lv et al. [10] studied the influence of pavement thickness, pavement elastic modulus, vehicle load, and vehicle impact force on pavement stress. Law and Zhu [11] systematically analysed the moving load on the vehicle-bridge system. The results showed that the theoretical solution method could identify the moving load independently and was superior to the finite element method. Liu et al. [12] compared and analysed the natural vibration characteristics of the actual corrugated steel web box girder and the general concrete web box girder, and the results showed that the torsional stiffness of the corrugated steel web box girder was low. A new diaphragm plate was proposed to improve the dynamic characteristics of torsion. Zheng [13, 14] studied the single-box multicell corrugated steel web box girder and concrete box girder by combining the modal test and finite element analysis and analysed the influence of the setting of diaphragm plates on torsional vibration frequency of the two box girders. Zhu and Wu [15] used the time-history analysis method to analyse the seismic response of the continuous rigid frame bridge with corrugated steel webs and the corresponding continuous rigid frame bridge with concrete webs and compared the structural displacement and internal force of the two models under longitudinal, transverse, and vertical earthquakes.

The research contents in the above literatures can be roughly divided into three types: (1) the static and dynamic response analysis of the concrete box girder bridge only, (2) the static and dynamic response analysis of the box girder bridge with corrugated steel webs only, and (3) comparison of the vibration characteristics and seismic performance of the box girder bridge with corrugated steel webs and equivalent concrete web box girder bridge. However, there is no literature comparing the dynamic response of the box girder bridge with corrugated steel webs and equivalent concrete web box girder bridge under moving loads. With the increasing use of box girder bridges, it is necessary to study the dynamic characteristics of box girder bridges. In this study, the three-dimensional finite element models of the superstructure of the corrugated steel web box girder bridge with the deck pavement and equivalent concrete web box girder bridge are established by using ABAQUS. The dynamic response of the pavement layer under different speeds and different load types is calculated, and the vertical displacement, longitudinal shear stress, and transverse stress of the two bridges are compared. It provides theoretical reference for further study of the dynamic response of the deck pavement system of box girder bridges.

2. Establishment of Finite Element Model

2.1. Model Description. The bridge is a box girder bridge with corrugated steel webs, the span of the bridge is 34 m, and the width of a single deck is 14 m. It adopts a single box and single chamber section. The height of the beam is 2 m, and the thicknesses of the top plate and bottom plate are all 25 cm. The wavelength of corrugated steel webs is 1.60 m, the wave height is 0.22 m, and the width of horizontal panels is 0.43 m. The horizontal folding angle is 30.7°, the bending radius is 0.24 m, and the thickness of corrugated steel webs is 16 mm. The top of the box girder is covered with 0.1 m thick C30 concrete. The box girder is only provided with longitudinal prestressed reinforcing steel. The top and bottom plates use C50 concrete, whose designed axial compressive strength is 22.4 MPa and designed axial tensile strength is 1.83 MPa. The corrugated steel web is made of Q345D steel. The prestressed reinforcing steel is a Φ^s15.24 steel strand with high strength and low relaxation, and it is arranged in the body.

The concrete web box girder bridge is constructed by using the principle of equivalent section. The thickness of the concrete web [10] is calculated according to the following formula:

$$t = \frac{[\tau_1]}{[\tau]} t_s, \tag{1}$$

where $[\tau_1]$ and $[\tau]$ represent the allowable shear strength of steel plates and concrete, the values of which are found by the specification, respectively, and t_s represents the thickness of the corrugated steel web.

Through calculation, the thickness of the concrete web is 450 mm. Dimensions of other parts of the beam and material parameters are the same as those of the box girder bridge with corrugated steel webs. The longitudinal elevation of the box girder bridge with corrugated steel webs is shown in Figure 1. The cross section of the main girder is shown in Figure 2. According to Chinese *JTGD 62-2004 Design Code for Highway Reinforced Concrete and Prestressed Concrete Bridges and Culverts* [16], the basic material parameters are obtained and are shown in Table 1.

2.2. Establishment of Finite Element Model. Because the two models differ only in the webs, the modeling method of the box girder bridge with concrete webs is similar to that of the box girder bridge with corrugated steel webs. The box girder and bridge deck pavement are all built by a 3D solid element and simulated by a C3D8R element. Corrugated steel webs are built by a shell element and simulated by an S4R element. The steel is built by a line element and simulated by a T3D2 element. In the Interaction module, Embedded is used to embed steel into concrete to form coupling constraints. The contact part between the bridge deck pavement and the box girder and the contact part between webs and the box girder is constrained by Tie (Tie in ABAQUS can simulate the connection between the two). The boundary of the box girder bridge is a movable hinge support at one end, which constrains the vertical and transverse displacement of the beam, and the other end is a fixed hinge support, which constrains the vertical, longitudinal, and transverse displacement of the beam. The concrete box girder bridge has a total of 76,540 units, of which 5,780 are wire units. The box girder bridge with corrugated steel webs has a total of 72,316 units, of which 2,016 are shell units and 5,100 are wire units. The established finite element models are shown in Figure 3. Figure 3(a) shows the finite element model of the whole bridge. Figures 3(b) and 3(c) show the detailed structural diagram of the two bridges, respectively.

2.3. Simplification of Vehicle Load. The actual tire landing size varies depending on tire pressure. For analysis and calculation, the ground contact area is a rectangular load. The influence of two different types of loads on the bridge deck pavement is considered separately: single wheel rectangular uniform load and double wheel rectangular uniform load. The size of each rectangle is $0.184\,\text{m} \times 0.2\,\text{m}$. The moving load is standard axle load BZZ-100 (rear axle) with a wheel load axle weight of 0.7 MPa. Considering the horizontal impact coefficient of 0.3, the value is 0.21 MPa, which is consistent with the direction of the moving load. From Figure 3, it can be seen that the meshes of the loading position (two load belts) are dense, while the meshes are gradually sparse in further distances. The DLOAD and UTRACLOAD subroutines are called by ABAQUS to move the load from one end of the bridge to the other. As time changes, the load rolls forward along a predefined path. The loading regions are shown in Figure 4.

3. Comparison and Analysis of Calculation Results

The pavement layer is above the concrete, so the vertical displacement of the pavement surface reflects not only the overall strength and stiffness of the pavement layer and concrete beam but also the performance of the pavement layer. The main factor of controlling the longitudinal crack of the pavement layer is the maximum transverse stress. The horizontal shear stress generated by a driving load is mainly concentrated in the range of 10 cm below the road surface. When the interlayer interface strength between layers is insufficient, horizontal displacement occurs between pavement layers. Therefore, the vertical displacement, longitudinal shear stress, and transverse stress of the pavement are analysed in this paper.

3.1. Comparison and Analysis of Natural Frequencies. In order to verify the correctness of the finite element model, the calculation formula [17] of the fundamental frequency of bridge vibration is given in the *CJJ 11-2011 Code for Design of the Municipal Bridge*:

$$f = \frac{13.616}{2\pi l^2}\sqrt{\frac{EI_c}{m}}, \tag{2}$$

where f represents the fundamental frequency of vibration, l represents the calculation span, I_c represents the cross-sectional moment of inertia, and m represents the midspan unit length mass.

An improved formula for solving the bending vibration frequency of the simply supported box girder bridge with corrugated steel webs is proposed in reference [18], as follows:

$$f = \frac{\sqrt{1 + \left(\left(5E_c b^2/112G_c\right)(\pi/l)^2\right)}\sqrt{IE_c/m}\,(\pi/l)^2}{2\pi\sqrt{1 + \left(5E_c b^2/14G_c\right)(\pi/l)^2 + \left(IE_c/G_s A_s\right)(\pi/l)^2 + \left(5IE_c^2 b^2/112G_c G_s A_s\right)(\pi/l)^4}}, \tag{3}$$

where E_c and G_c represent the elastic modulus and shear modulus of concrete, respectively; b represents half of the clear span of the wing plate in the box; and A_s represents the shear area of corrugated steel webs.

The vibration frequency calculated (Table 2) by the finite element method of ABAQUS is compared with the calculated values of 3.740 and 2.8529 of equations (2) and (3). The error between them is small, which verifies the correctness of the finite element model.

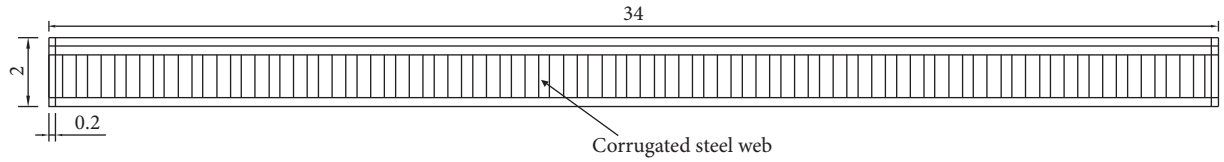

Figure 1: Longitudinal elevation of the box girder bridge with corrugated steel webs (unit: m).

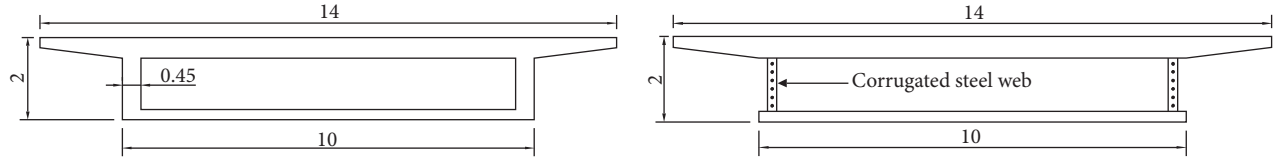

Figure 2: Cross section of the main girder (unit: m). (a) Concrete box girder. (b) Box girder with corrugated steel webs.

Table 1: Basic material parameters.

Pavement architecture	Elastic modulus (MPa)	Poisson's ratio	Density (kg·m^{-3})	Coefficient of linear expansion (K^{-1})	Damping ratio
C30 concrete	3.0×10^4	0.2	2400	1.0×10^{-5}	0.05
C50 concrete	3.45×10^4	0.2	2500	1.0×10^{-5}	0.05
Φ^s15.24 stranded wire	2.0×10^5	0.3	7800	1.0×10^{-5}	0.05
Q345D steel	2.1×10^5	0.3	7850	1.0×10^{-5}	0.05

The following conclusions can be drawn from Table 2 and Figure 5:

(1) The natural frequency of the CSWBG bridge is less than that of the CWBG bridge, which shows that the CSWBG bridge has good seismic performance.

(2) The first-order mode of both the CSWBG bridge and the CWBG bridge is vertical bending, indicating that the vertical stiffness of both bridges is less than the transverse stiffness and longitudinal stiffness.

(3) The second-order mode of both the CSWBG bridge and the CWBG bridge is torsional, and the frequency of the CSWBG bridge is small, which indicates that the torsional stiffness is low. The reason is that the vertical and transverse stiffness of the CSWBG bridge is mostly provided by the concrete top and bottom plates. However, the webs of the box girder with corrugated steel webs are thin, and the frame effect of torsional resistance is not as obvious as that of the ordinary box girder with concrete webs, which results in low torsional stiffness.

3.2. Comparison and Analysis of Bridge Deck Pavement Response under Different Load Types

3.2.1. Comparison of Vertical Displacement on the Surface of Bridge Deck Pavement under Different Load Types. Figures 6 and 7 show the results of vertical displacement and maximum vertical displacement on the surface of the bridge deck pavement of both models under single wheel rectangular load and double wheel rectangular load, when the speed is 108 km/h.

Figure 6 indicates that the maximum deflection of both bridges occurs at or near the middle of the span under single wheel rectangular load and double wheel rectangular load, when the speed is 108 km/h. Each curve has a similar trend and moves forward in a wavy shape. It can be seen from Figure 7 that, under the same conditions, the maximum vertical displacement on the surface of the bridge deck pavement of the CSWBG bridge is larger than that of the CWBG bridge, and the change of load type has more obvious influence on the maximum vertical displacement of the bridge deck surface of the CSWBG bridge.

3.2.2. Comparison of Longitudinal Shear Stress between Layers of Bridge Deck Pavement under Different Load Types. Figure 8 shows the results of the longitudinal shear stress between layers of the bridge deck pavement of both models under single wheel rectangular load and double wheel rectangular load, when the speed is 108 km/h.

It can be seen from Figure 8 that the maximum longitudinal shear stress between layers appears near the middle of the span under rectangular load, and the trend of each curve is similar. It can be observed from Figures 8(a) and 8(b) that when the speed is the same, the maximum longitudinal shear stress between layers of two bridges under double wheel rectangular load is greater. It can be found from Figures 8(c) and 8(d) that when the speed and load

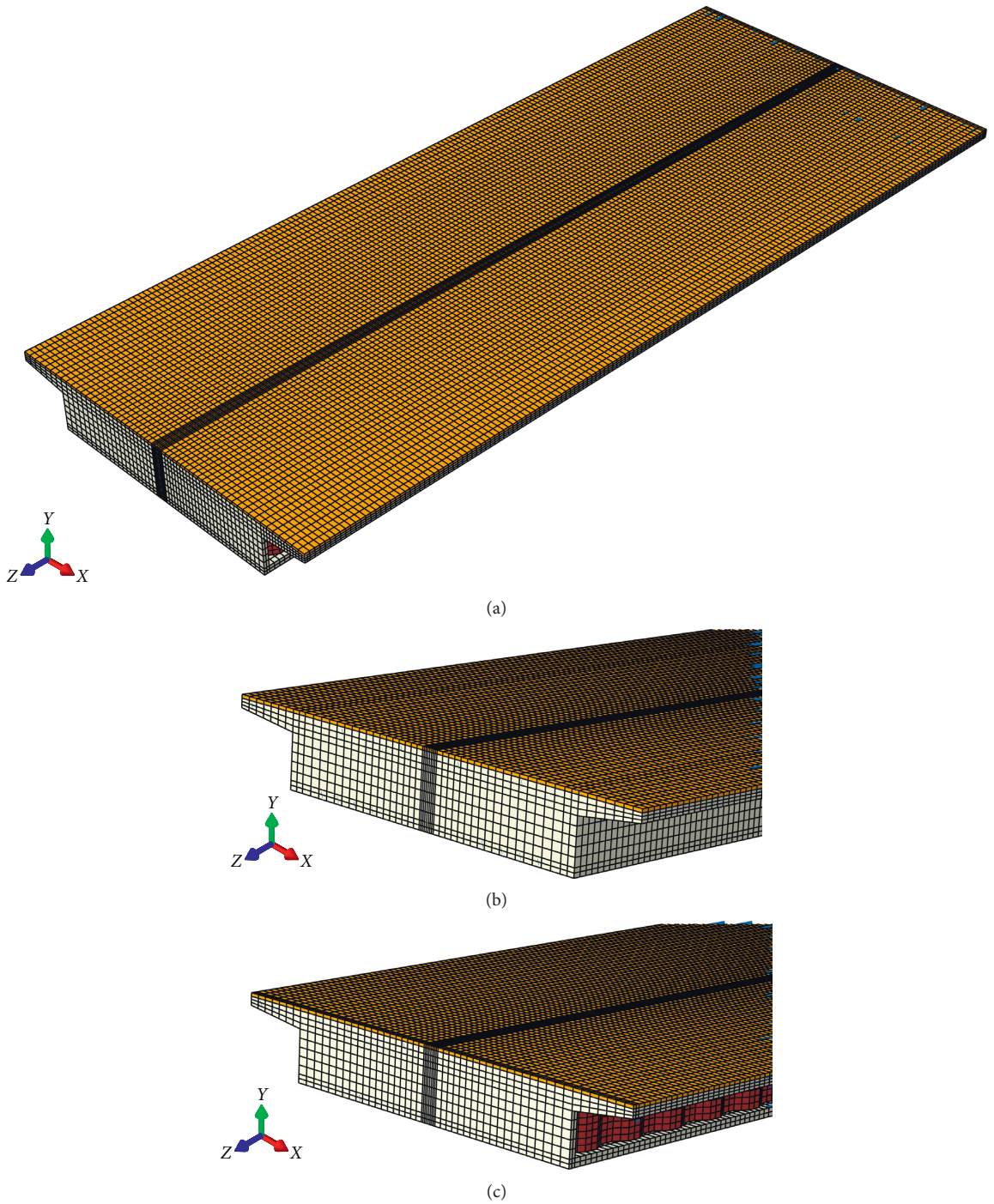

Figure 3: Finite element model of the bridge deck pavement. (a) Finite element model of the whole bridge. (b) Paving model of the concrete web box girder bridge. (c) Paving model of the box girder bridge with corrugated steel webs.

types are the same, the maximum longitudinal shear stress between the CWBG bridge and the CSWBG bridge is basically the same.

3.2.3. Comparison of Transverse Stress on the Surface of Bridge Deck Pavement under Different Load Types. Figures 9 and 10 show the results of the transverse stress and maximum transverse stress on the surface of the bridge deck pavement of both models under single wheel rectangular load and double wheel rectangular load, when the speed is 108 km/h.

Figure 9 illustrates that the maximum transverse stress of both bridges occurs at or near the middle of the span under single wheel rectangular load and double wheel rectangular load, when the speed is 108 km/h. The trend of each curve is similar. It can be found from Figure 10 that the maximum transverse stress on the surface of the bridge deck pavement

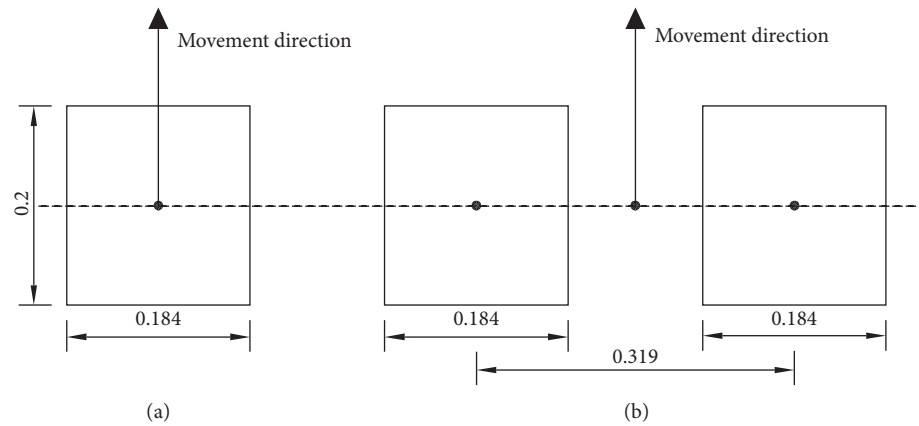

Figure 4: Rectangular load area. (a) Single wheel rectangular load. (b) Double wheel rectangular load.

Table 2: Comparison of the first 10 natural frequencies of the two models.

	CWBG bridge	CSWBG bridge
1	3.2980	2.9816
2	8.2043	6.0808
3	8.7369	6.7948
4	9.9666	7.4979
5	10.713	8.5938
6	11.972	10.001
7	12.775	10.700
8	14.178	11.540
9	14.560	12.777
10	15.620	14.205

Note: the CWBG bridge means the concrete web box girder bridge, and the CSWBG bridge means the corrugated steel web box girder bridge.

of the CSWBG bridge is larger than that of the CWBG bridge under the same conditions, and the change of load type has more obvious effect on the maximum transverse stress on the surface of the deck pavement of the CSWBG bridge.

3.3. Comparison and Analysis of Bridge Deck Pavement Response under Different Speeds

3.3.1. Comparison of Vertical Displacement on the Surface of Bridge Deck Pavement under Different Speeds. Figures 11 and 12 show the results of the vertical displacement and maximum vertical displacement on the surface of the bridge deck pavement of both models under double wheel rectangular load at different speeds.

It can be seen from Figure 11 that the maximum deflection of the two bridges occurs at or near the middle of the span under double wheel rectangular load, when the speed is different. Each curve has a similar trend and moves forward in a wavy shape. Figure 12 shows that the vertical displacement on the surface of the bridge deck pavement of both models increases gradually with the increase of moving load speed. Under the same conditions, the maximum vertical displacement on the surface of the bridge deck pavement of the CSWBG bridge is larger than that of the CWBG bridge, and the change of speed has a more obvious effect on the maximum vertical displacement on the surface of the deck pavement of the CSWBG bridge.

3.3.2. Comparison of Longitudinal Shear Stress between Layers of Bridge Deck Pavement under Different Speeds. Figure 13 shows the results of the longitudinal shear stress between layers of the bridge deck pavement of both models under double wheel rectangular load. Figures 13(a) and 13(b) show the results of the longitudinal shear stress between layers of the bridge deck pavement under double wheel rectangular load at different speeds. Figures 13(c)–13(e) show the results of the longitudinal shear stress between layers of the bridge deck pavement under double wheel rectangular load at the same speed.

It can be seen from Figure 13 that the maximum longitudinal shear stress between layers appears near the middle of the span under double wheel rectangular load, and the trend of each curve is similar. It can be seen from Figures 13(a) and 13(b) that the effect of a velocity change on the maximum longitudinal shear stress between the CSWB bridge and the CSWBG bridge is consistent. Taking the CSWB bridge as an example, the maximum longitudinal shear stress values are basically the same at 36 km/h and 108 km/h. The maximum longitudinal shear stress at 72 km/h is small. It can be seen from Figures 13(c)–13(e) that when

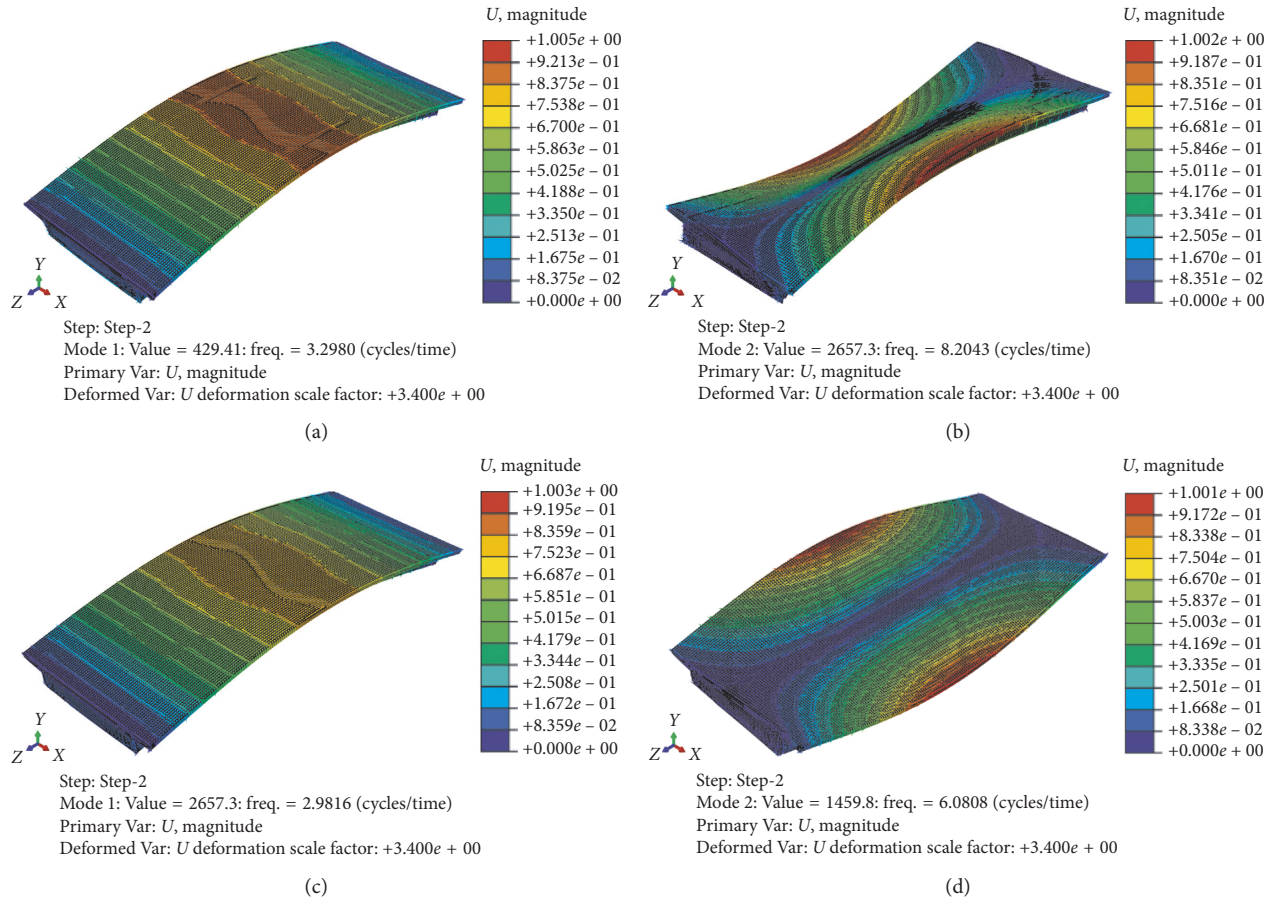

FIGURE 5: The first two modes of the two models. (a) The first-order mode and (b) the second-order mode of the CWBG bridge. (c) The first-order mode and (d) the second-order mode of the CSWBG bridge. CWBG: concrete web box girder; CSWBG: corrugated steel web box girder.

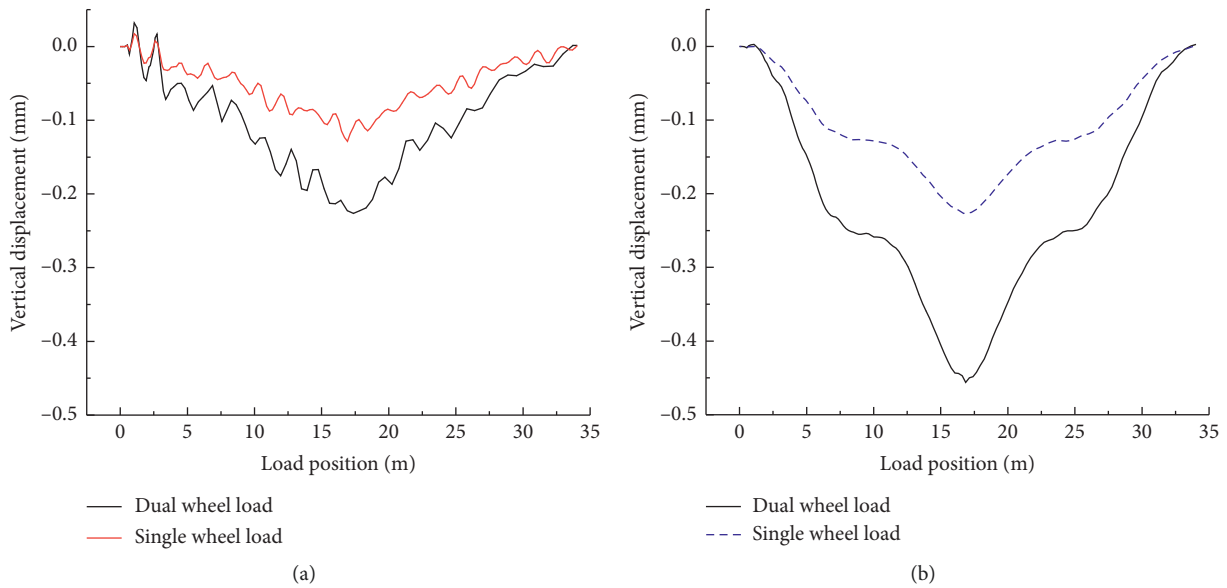

FIGURE 6: Comparison of vertical displacement on the surface of the bridge deck pavement of both models. (a) CWBG bridge. (b) CSWBG bridge.

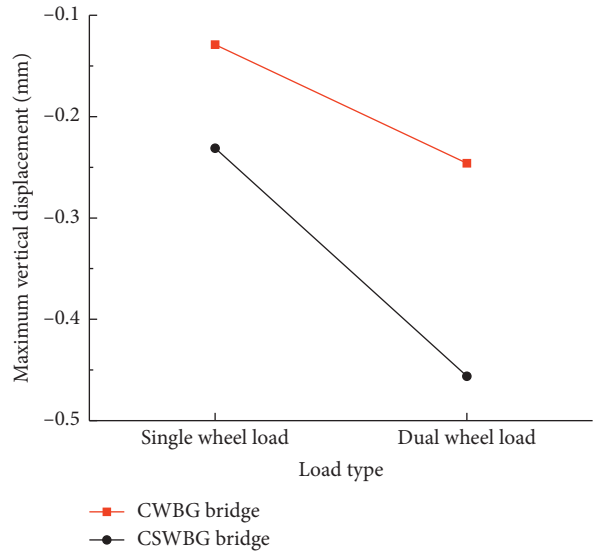

Figure 7: Comparison of maximum vertical displacement on the surface of the bridge deck pavement at the same speed.

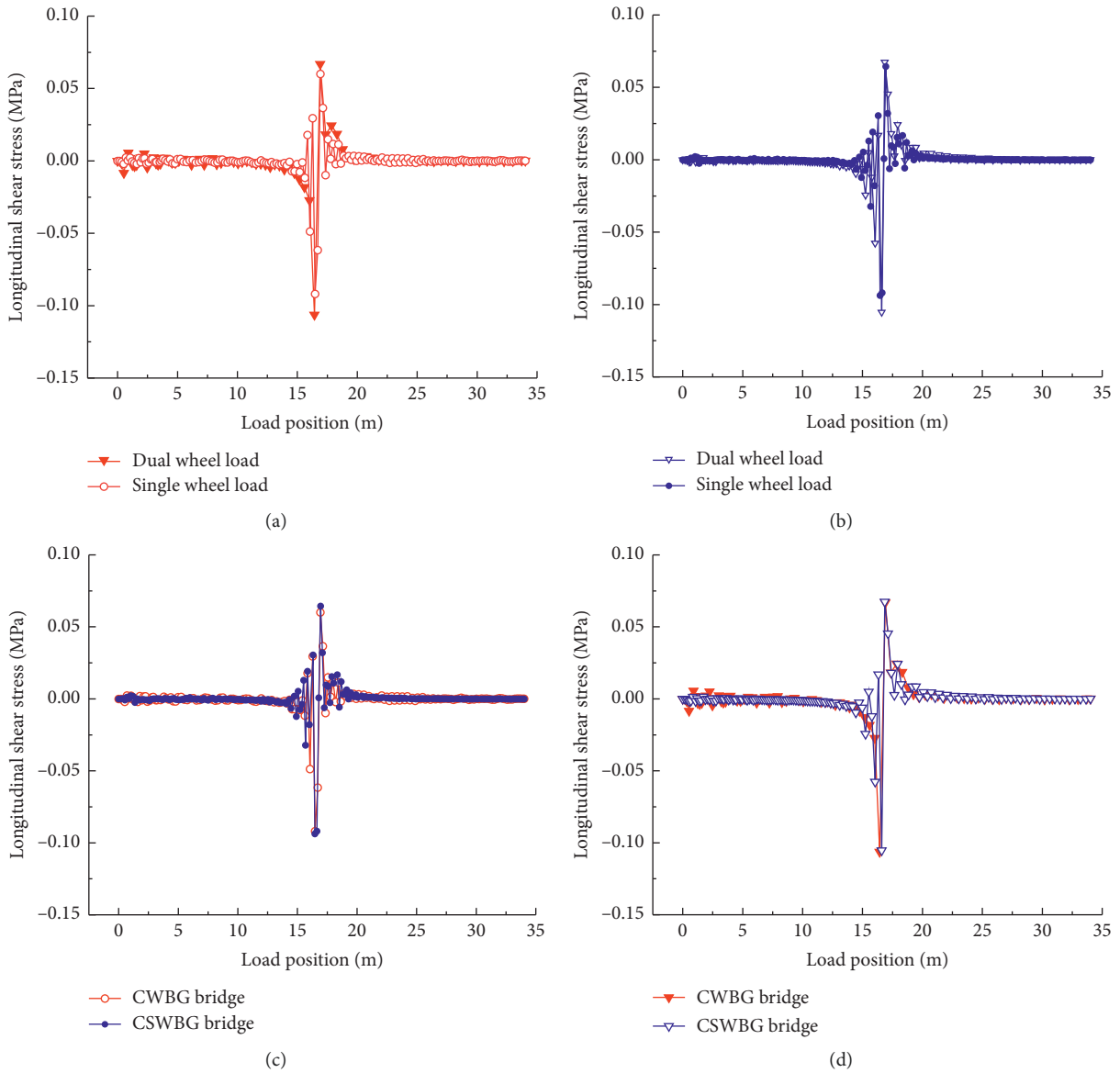

Figure 8: Comparison of longitudinal shear stress between layers of the bridge deck pavement of both models. (a) CWBG bridge. (b) CSWBG bridge. (c) Single wheel load. (d) Dual wheel load.

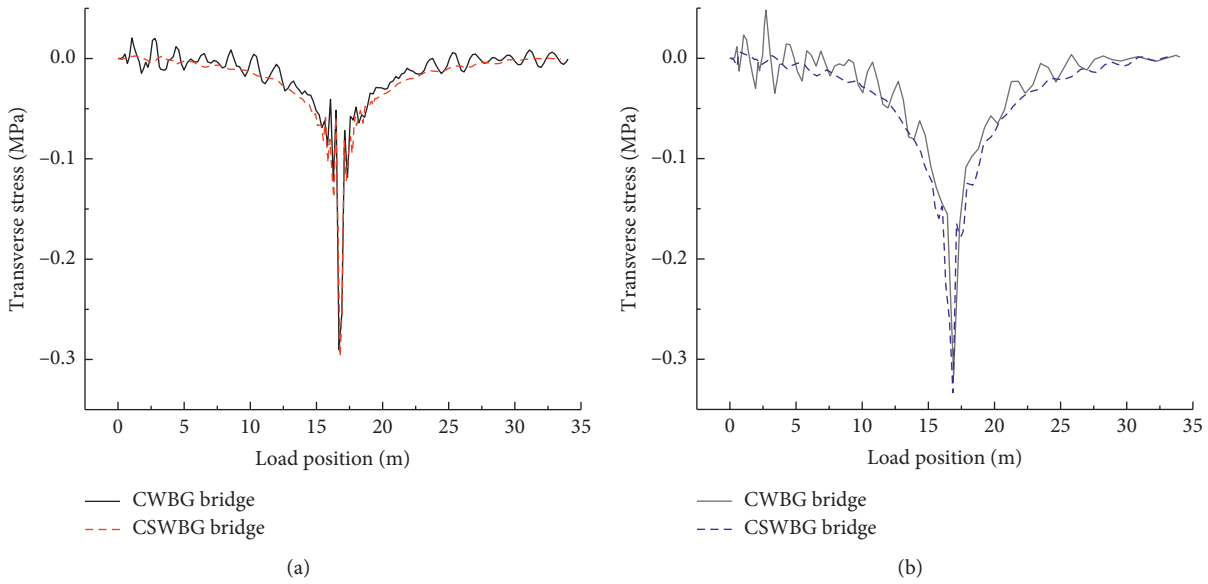

Figure 9: Comparison of transverse stress on the surface of the bridge deck pavement of both models. (a) Single wheel load. (b) Dual wheel load.

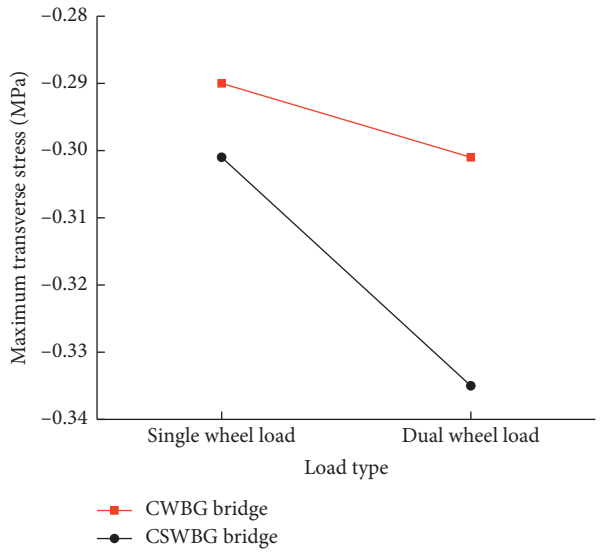

Figure 10: Comparison of maximum transverse stress on the surface of the bridge deck pavement at the same speed.

the load type is the same, the maximum longitudinal shear stress between layers of the CSWBG bridge is greater than that of the CWBG bridge under low speed and the maximum longitudinal shear stress between the two bridges is basically the same under high speed.

3.3.3. Comparison of Transverse Stress on the Surface of Bridge Deck Pavement under Different Speeds. The curve trend of the transverse stress contrast diagram of the surface of the bridge deck pavement under different speeds is similar to that of the surface of the bridge deck pavement under different load types, which is not repeated here, but only compared in Figure 14. It can be seen that the transverse stress on the surface of the bridge deck pavement of both models increases gradually with the increase of moving load speed, and the change of speed has a more obvious effect on the maximum transverse stress on the surface of the deck pavement of the CSWBG bridge.

4. Conclusions

This study analysed the difference of dynamic response of the deck pavement between the box girder bridge with corrugated steel webs and the concrete web box girder bridge. The displacement and stress of the deck pavement of two different bridges were compared and analysed. The following conclusions are drawn from this study:

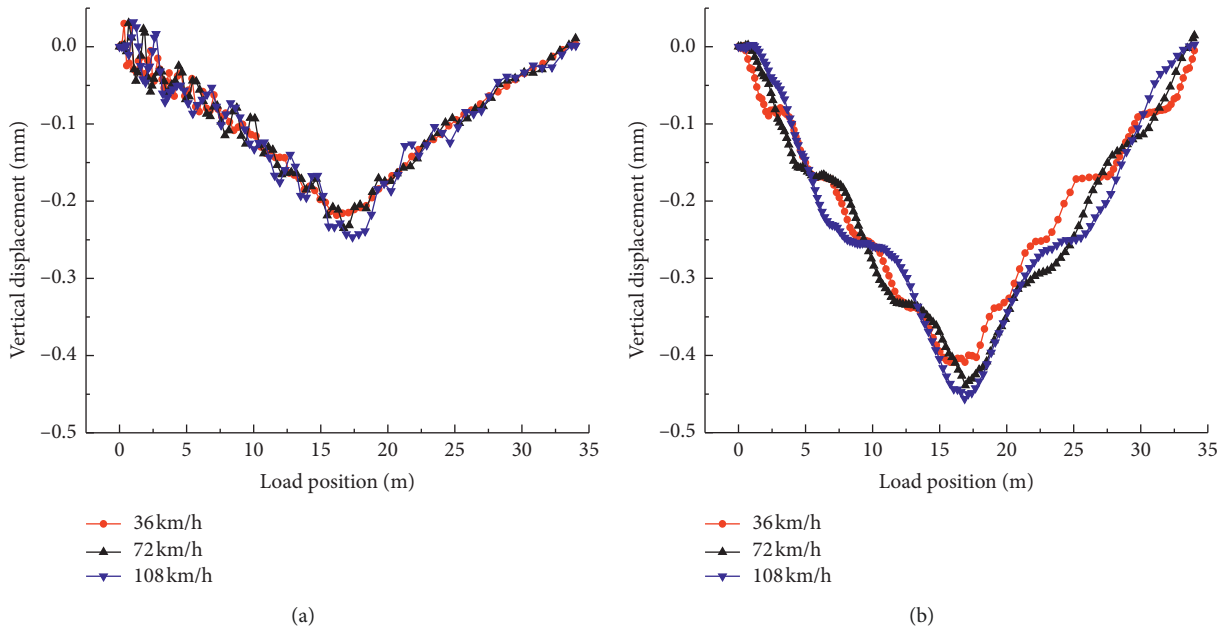

Figure 11: Comparison of vertical displacement on the surface of the bridge deck pavement of both models. (a) CWBG bridge. (b) CSWBG bridge.

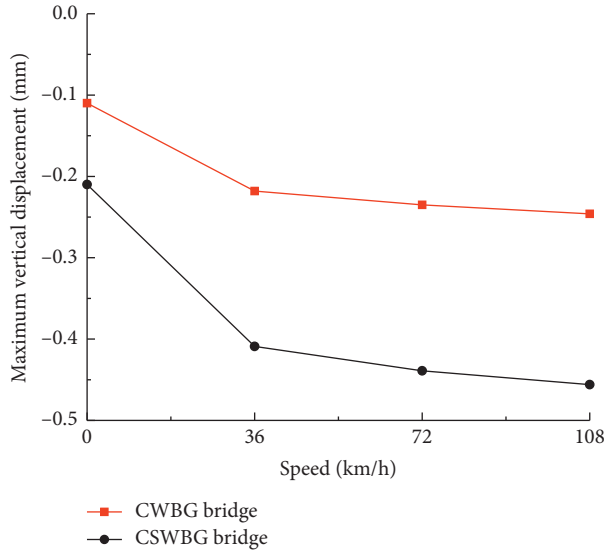

Figure 12: Comparison of maximum vertical displacement on the surface of the bridge deck pavement under double wheel load.

(1) When the area and other conditions are the same, the bending moment of a concrete beam is mainly borne by top and bottom plates, and the overall bending resistance of the section is improved. The maximum vertical displacement of the CSWBG bridge pavement layer is larger than that of the equivalent CWBG bridge, which is more affected by the change of load type and speed. It indicates that the CSWBG bridge has lightweight, good bending resistance, and more obvious advantages in deflection control.

(2) When the stiffness of the bridge deck system is small or local stiffness difference is large, the excessive vertical deformation of the bridge deck would lead to large shear stress under the same load. Under the same condition, the maximum longitudinal shear stress between layers of the CSWBG bridge deck pavement is larger than that of the equivalent CWBG bridge. It indicates that webs have an influence on longitudinal shear stress between layers of the pavement, and the stiffness of the CSWBG bridge pavement should be increased to prevent the damage of the adhesive layer.

(3) The transverse stiffness of the CSWBG bridge is mainly borne by the roof and bottom plate.

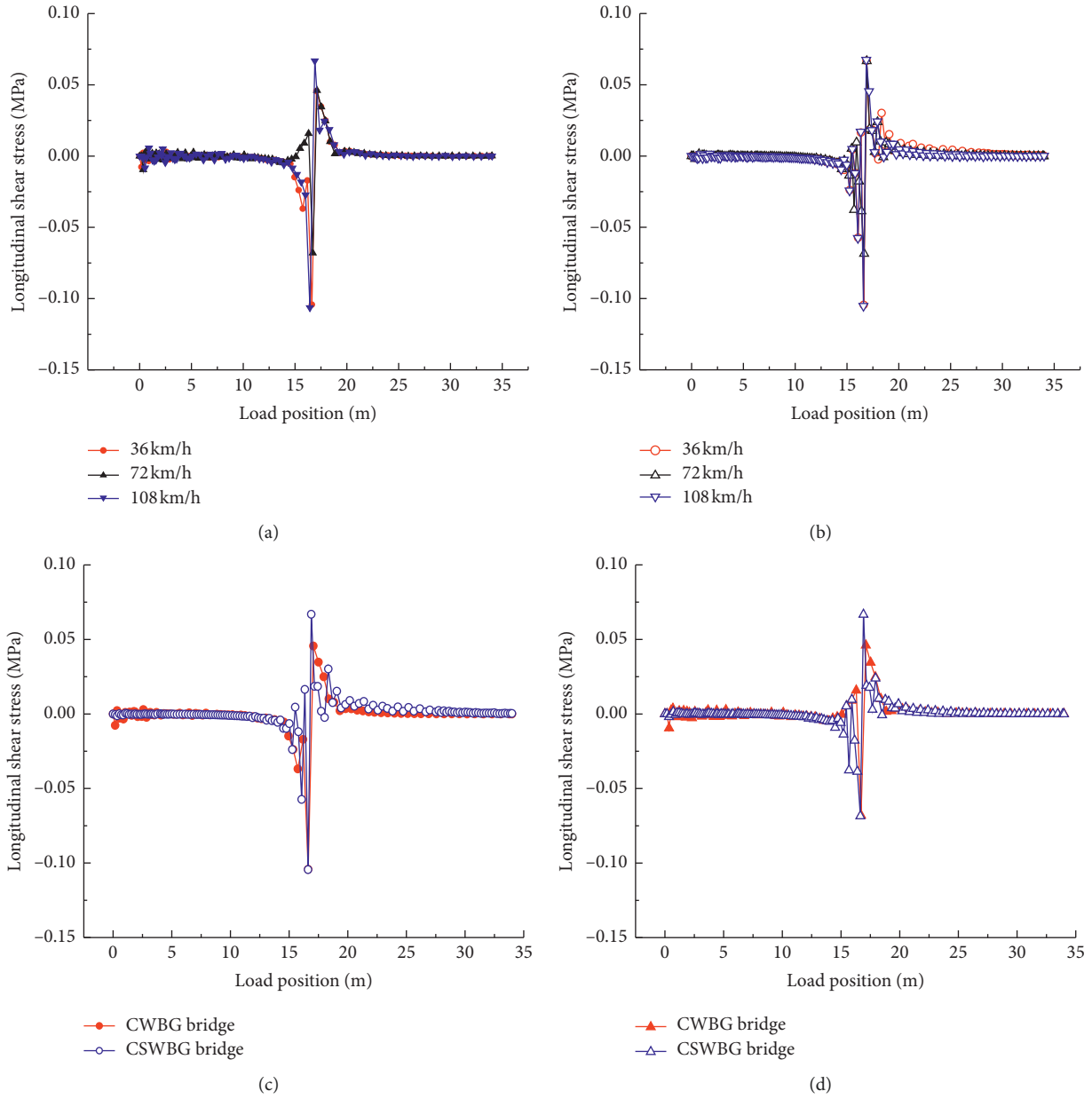

Figure 13: Continued.

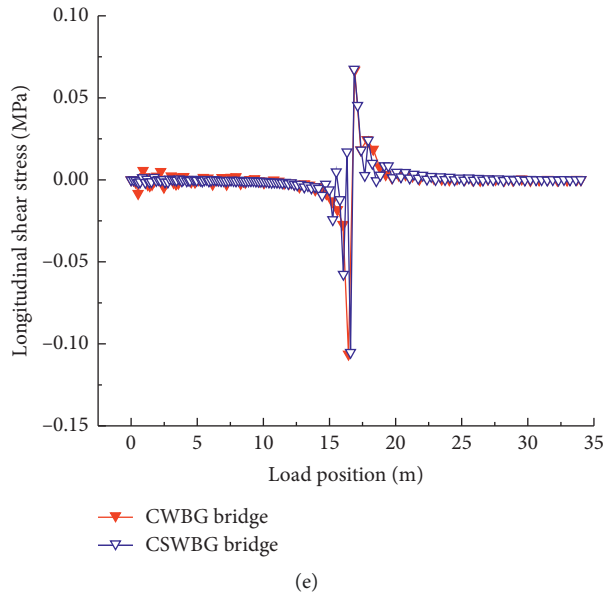

Figure 13: Comparison of longitudinal shear stress between layers of the bridge deck pavement of both models. (a) CWBG bridge. (b) CSWBG bridge. (c) 36 km/h. (d) 72 km/h. (e) 108 km/h.

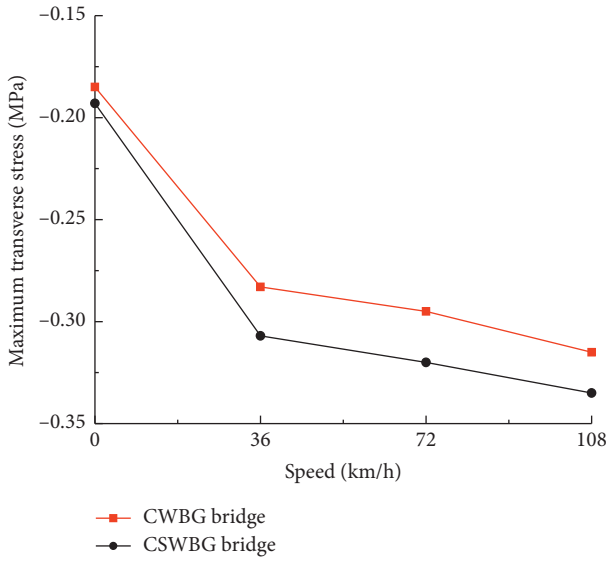

Figure 14: Comparison of maximum transverse stress on the surface of the bridge deck pavement under double wheel load.

Compared with the equivalent CWBG bridge, transverse bending stiffness of the CSWBG bridge is smaller. Under the same condition, the maximum transverse stress of the CSWBG bridge pavement layer is larger than that of the equivalent CWBG bridge, and it is more obviously affected by the change of load type and speed. It indicates that the transverse diaphragm plate should be properly configured in the CSWBG bridge to improve the effective torsional stiffness of the box girder so as to facilitate lateral stiffness distribution.

(4) The stiffness and self-weight of the box girder bridge with corrugated steel webs are small, so the dynamic interaction of the axle is more obvious under the action of the vehicle.

Data Availability

The data used to support the findings of this study are available from the corresponding author upon request.

Conflicts of Interest

The authors declare no conflicts of interest.

Acknowledgments

This research was funded by the National Natural Science Foundation of China (grants 11202142, 11872555, and 11872253), the Science and Technology Plan Project of Hebei Qugang Expressway Development Co., Ltd. (QG 2018-07), and the Funded Project of Returned Overseas Personnel (C20190513).

References

[1] M. Castro, "Structural design of asphalt pavement on concrete bridges," *Canadian Journal of Civil Engineering*, vol. 31, no. 4, pp. 695–702, 2004.

[2] A. Fiore and G. C. Marano, "Service ability performance analysis of concrete box girder bridges under traffic-induced vibrations by structural health monitoring: a case study," *International Journal of Civil Engineering*, vol. 16, no. 5, pp. 553–565, 2018.

[3] W. Choi, I. Mohseni, J. Park, and J. Kang, "Development of live load distribution factor equation for concrete multicell box-girder bridges under vehicle loading," *International Journal of Concrete Structures and Materials*, vol. 13, no. 1, pp. 1–14, 2019.

[4] L. Sang-Youl and Y. Sung-Soon, "Dynamic behavior of long-span box girder bridges subjected to moving loads: numerical analysis and experimental verification," *International Journal of Solids and Structures*, vol. 42, no. 18-19, pp. 5021–5035, 2005.

[5] T. J. Du, *Finite Element Analysis of Deck Pavement of Reinforced Concrete Box Girder Bridge*, Dalian University of Technology, Dalian, China, 2011.

[6] T. J. Du and J. Y. Chen, "Dynamic finite element analysis of asphalt concrete deck pavement," *Northern Communications*, vol. 9, pp. 28–32, 2011.

[7] I. Mohseni, A. R. Khalim, and E. Nikbakht, "Effectiveness of skewness on dynamic impact factor of concrete mulicetll box-girder bridges subjected to truck loads," *Arabian Journal for Science and Engineering*, vol. 39, no. 8, pp. 6083–6097, 2014.

[8] K. H. Jung, J. W. Yi, and J. H. J. Kim, "Structural safety and serviceability evaluations of prestressed concrete hybrid bridge girders with corrugated or steel truss web members," *Engineering Structures*, vol. 32, no. 12, pp. 3866–3878, 2010.

[9] H.-J. Ko, J. Moon, Y.-W. Shin, and H.-E. Lee, "Non-linear analyses model for composite box-girders with corrugated steel webs under torsion," *Steel and Composite Structures*, vol. 14, no. 5, pp. 409–429, 2013.

[10] G. B. Lv, L. Yang, J. Q. Han et al., "Analysis on mechanical properties of PC composite box girder bridge with corrugated steel webs," *Journal of Xihua University (Natural Science)*, vol. 3, no. 36, pp. 96–101, 2017.

[11] S. S. Law and X. Q. Zhu, "Damage detection in simply supported concrete bridge structure under moving vehicular loads," *Journal of Vibration and Acoustics*, vol. 129, no. 1, pp. 58–65, 2007.

[12] B. D. Liu, H. B. Chen, and H. W. Ren, "Study on improvement of dynamic characteristics of corrugated steel web concrete box girder," *China Railway Science*, vol. 3, pp. 29–33, 2008.

[13] S. M. Zheng, *Study on Dynamic Performance of PC Composite Box Girder Bridge with Corrugated Steel Webs*, Southeast University, Nanjing, China, 2016.

[14] S. M. Zheng, S. Wan, and H. G. Cheng, "Study on dynamic characteristics of single box multi-chamber corrugated steel web composite box girder," *Journal of Railway Engineering*, vol. 34, no. 9, pp. 41–46, 2017.

[15] B. Zhu and X. H. Wu, "Dynamic characteristics and seismic performance analysis of continuous rigid frame bridges with corrugated steel webs," *East China Highway*, no.2, Article ID 1001-7291(2017)02-0015-03, pp. 15–17, 2017.

[16] People's Traffic Press, *JTGD 62-2004 Design Code for Highway Reinforced Concrete and Prestressed Concrete Bridges and Culverts*, People's Traffic Press, Beijing, China, 2004.

[17] China Building Industry Press, *CJJ 11-2011 Code for Design of the Municipal Bridge*, China Building Industry Press, Beijing, China, 2011.

[18] W. Ji, S. Liu, and P. Z. Lin, "Vibration frequency analysis and test of corrugated steel web composite box girder," *China Highway Journal*, vol. 26, no. 5, pp. 102–107, 2013.